Int. J. Heat Mass Transfer. Vol. 26, No. 9, pp. 1307–1320, 1983
Printed in Great Britain

0017-9310/83 $3.00 + 0.00

HEAT TRANSFER IN LARGE PARTICLE FLUIDIZED BEDS

N. DECKER* and L. R. GLICKSMAN
Department of Mechanical Engineering, Massachusetts Institute of Technology, Cambridge, MA 02139, U.S.A.

(*Received* 23 *September* 1981 *and in final form* 6 *January* 1983)

Abstract—A physically based model is proposed for heat transfer to immersed surfaces in large particle fluidized beds. 'Large' particles are distinguished as those with thermal time constants substantially greater than their residence time at a heat transfer surface. At typical fluidized bed combustor operating conditions, particles 1 mm or larger are 'large'. Conduction through the gas near points of solid contact and convection by the interstitial gas flow both contribute to heat transfer during emulsion (or dense phase) contact. As particle size increases the heat transfer by gas convection provides a greater share of the heat transfer. It is shown that the gas convective component in fluidized bed heat transfer is not simply related to overall gas convection in a packed or quiescently fluidized bed. The model is shown to provide good agreement with data from several sources.

NOMENCLATURE

c	specific heat of gas
c_s	specific heat of particle
d_p	particle diameter
f_0	fraction of time voids reside at surface
h	heat transfer coefficient
h_b	heat transfer coefficient under bubble or void
$h_{conduction}$	heat transfer coefficient by conduction in region near contact point
h_e	heat transfer coefficient under emulsion
k	thermal conductivity of particle
k_e	effective thermal conductivity of emulsion
k_g	thermal conductivity of gas
l_0	length in flow direction for estimate of convection near point of contact
$q_{conduction}$	rate of heat transfer by conduction in region near contact point
t_r	mean residence time of particle at surface
T_B	bulk bed temperature
T_I	intermediate temperature at interface
T_w	wall or surface temperature
U	superficial velocity of gas
U_B	bubble rise velocity
U_{mf}	minimum fluidization velocity
v_0	effective mean velocity in convection estimate
w_0	mean spacing used in estimate of convection near contact point
y	local normal distance from heat transfer surface to particle surface

Greek symbols

δ	bubble voidage
ε_{mf}	voidage at minimum fluidization
ν	gas kinematic viscosity
ρ	gas density
ρ_s	particle density
τ	thermal time constant of particle at surface
ϕ	angular dimension of region considered in convection estimate

Non-dimensional

Ar	Archimedes number, $gd_p^3(\rho_s-\rho)/\rho\nu^2$
Bi	Biot modulus, $hd_p/2k$
Nu	Nusselt number, hd_p/k_g
Pr	Prandtl number, $\nu\rho c/k_g$
Re	Reynolds number, Ud_p/ν

1. INTRODUCTION

THERE has been an increased interest in the behavior of fluidized beds made up of large particles for applications such as fluidized bed combustors. However, most of the published work on heat transfer to surfaces immersed in fluidized beds has dealt with beds of small particles. Attempts to extrapolate results derived for small particles to large particles have been unsatisfactory. In many instances the heat transfer behavior of small and large particles are contradictory. For example, the heat transfer coefficient h, decreases rapidly as the average diameter of small particle systems is increased. On the other hand, with large particle systems h has been observed, in some instances, to increase with particle diameter. Heat transfer in small particle systems is unaffected by changes in the pressure level, whereas h increases rapidly as the pressure level is raised in beds with large particles.

The differences in the observed trends stem from the existence of more than a single mechanism of heat transfer. In addition, there is a shift of dominance from one mechanism to another as solid properties and fluidizing conditions are altered. Physically based models with clearly defined limits of applicability are required for the proper interpretation of experimental results and the prediction of situations yet untested.

* Present address: Dept. of Mechanical Engineering, University of Minnesota, 111 Church Street S.E., Minneapolis, MN 55455, U.S.A.

A physical model of heat transfer for large particles is presented here. The principle mechanisms are described along with a consideration of the conditions under which each mechanism is important. This will lead to a simplified prediction of the heat transfer in large particle fluidized beds.

2. LARGE PARTICLES

The study of heat transfer in large particle beds will be facilitated by an estimation of the thermal time constant, τ, of an individual particle immediately adjacent to the heat transfer surface. To establish an estimate for τ we must anticipate results to be presented later. Consider the first layer of particles at the surface. At ambient temperatures, the primary mechanism for heat transfer with the wall is conduction through the gas. Based on a detailed model of the particle-to-surface bubble frequencies are 1 Hz or greater [2] in an open bed will be 1/24 of the particle diameter or larger [1]. The average heat transfer coefficient between the particle and the wall is 24 k_g/d_p. The Biot modulus becomes

$$Bi = 12\frac{k_g}{k}. \tag{1}$$

For limestone particles in air Bi is approximately 0.25, for metal particles in air Bi is still smaller.

A small value of Bi, which relates gas film resistance to the conduction resistance through the particle indicates that on the average, the temperature difference within the particle is negligible compared to that between the particle and the heat transfer surface. The particle can be assumed to be at a uniform temperature and the thermal time constant can be estimated as

$$\tau \sim \frac{1}{36}\frac{\rho_s c_s d_p^2}{k_g}. \tag{2}$$

The value of τ is based on the lower limit of the conduction path, $d_p/24$; thus it represents a lower limit on the thermal time constant. The value of τ is shown in Fig. 1 for three values of $\rho_s c_s/k_g$ ranging from limestone fluidized in ambient air to limestone fluidized at a film temperature of 1000°F.

The criterion for 'large particles' as used in this work is that the particle thermal time constant is much larger than the particle residence time. Typically, measured bubble frequencies are 1 Hz or greater [2] in an open bed even for superficial velocities close to the minimum fluidization velocity. Similar values of bubble or replacement frequency have been measured near tubes [3, 4]. Thus, when a freely bubbling bed contains particles 1 mm in diameter or larger, the thermal time constant of the particles is much larger than the replacement time. The average temperature of the particles does not change appreciably and the thermal interaction is confined to the region between the heat transfer surface and the first layer of particles. The heat transfer between individual particles, the wall, and the flowing gas in this region controls the overall surface heat transfer coefficient. Since the large particles do not change temperature significantly when they are at the wall, the exact value of the particle residence time is not required in the prediction of the heat transfer coefficient. This is in contrast with models for smaller particles such as that of Chandran [5] which require an explicit value of the residence time.

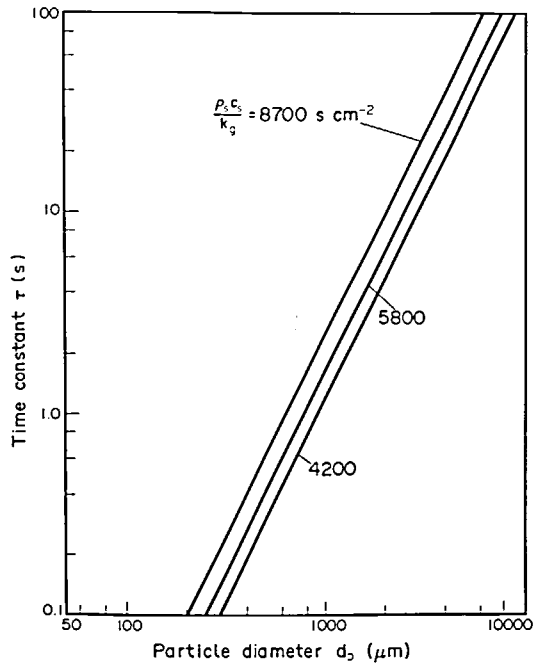

FIG. 1. Variation of particle thermal time constant with particle diameter.

3. OVERALL HEAT TRANSFER MODEL

Consider a surface immersed in a well-fluidized bed of large particles. At any time a portion of the surface is covered with particles, the balance of the surface is covered with gas voids. The temperature of the large particles can be taken equal to the bulk bed temperature. The average heat transfer over the entire surface is the sum of the heat transfer from the particles to the surface and the heat transfer from the gas voids to the surface weighted by the appropriate factors to account for the fraction of the surface covered by particles and voids, respectively [6]. At low temperatures, the particle heat transfer will consist of two effects: the conduction heat transfer near the point of contact between particles and surface and convection augmentation due to lateral mixing of the gas in the large voids between individual particles in the emulsion. At elevated temperatures effects of radiation must also be included. Each of these effects will be considered separately. By combining them together an overall prediction for large particle fluidized beds can be achieved.

4. CONDUCTION HEAT TRANSFER BETWEEN PARTICLE AND HEAT TRANSFER SURFACE

Conduction heat transfer will be concentrated in the regions where the separation between the particle and wall is small, i.e. near the point of contact. Consider the heat transfer between a single particle and the wall at temperatures T_B and T_w respectively. Idealizing the particle as spherical and the wall planar, then the conduction through the gas layer separating them can be expressed as

$$q_{\text{conduction}} = \int_0^{d_p/2} \frac{k_g}{y}(T_B - T_w)2\pi r \, dr \qquad (3)$$

where y is the local distance between the wall and the particle surface. We have assumed that the heat flow vector is always perpendicular to the wall. If the particle touches the wall for the idealized geometry of a sphere in point contact with a plane, the integral in equation (3), taken over the entire particle projected area, yields a singularity. Actually this singularity does not develop except for an infinitesimal period, after which the local temperature difference has been reduced. Schlünder [7] has argued that the region of gas within a small finite radius of the contact point has a conduction length y less than the mean free path of the gas molecules. Within this small neighborhood of the contact point the local gas conduction is reduced, eliminating the singularity. Heat transfer by solid-to-solid contact, however, is assumed negligible in his theory.

In two other investigations [8, 9] numerical methods have been employed to determine the temperature distribution within a particle as a function of time during the particle's residence at a surface of different temperature. Each modelled the contact point as a contact between a perfect sphere and a plane, and each found that their numerical estimates for the local heat flux considerably exceeded experimentally observed values. Both resorted to separating the particles from the wall by a fraction of the particle diameter to match experimental data, although Gabor [9] doubted the existence of such a separating layer of gas.

It is likely that many particles do touch the wall. However, to properly account for heat transfer near the contact point, a more realistic representation of the surface geometry is required. Near the contact region, the surface microstructure must be considered. Surfaces have microscopic roughness elements and there are relatively few actual solid-to-solid contact points when surfaces are brought together at low contact pressures typical of fluidized beds. Furthermore the roughness dimensions are typically much larger than the mean free path of gas molecules, thus ruling out the latter effect as a primary influence on the singularity near the contact point.

The analysis of the heat transfer in the contact region is dealt with in detail in a recent paper by the present authors [1]. It is shown that the overall particle-to-wall conduction is a moderate function of the surface roughness and a weak function of solid conductivity even for materials with very high conductivity, such as copper or aluminum. Figure 2 summarizes the results. The exact prediction of conduction requires detailed knowledge of particle and surface roughness geometry and particle arrangement at the wall. Given the limits on roughness for typical surfaces ranging from 10^{-2} to 10^{-4} mm an average value can be taken as

$$h_{\text{conduction}} = \frac{12 k_g}{d_p}. \qquad (4)$$

This value applies to particles with sphericity near

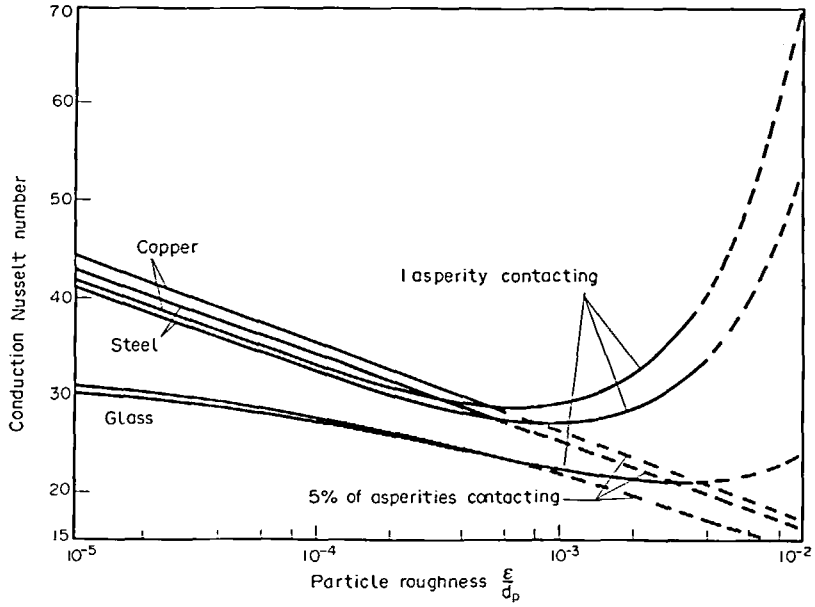

FIG. 2. Conduction Nusselt number variation with particle roughness for copper, steel, and glass particles with two different assumed contact arrangements.

unity. For irregular shaped particles the value of conduction resistances should be approximately halved. Recently, Gloski [10] has carried out measurements of the thermal resistance between a heat transfer surface and adjacent particles for both packed and fluidized beds. His results confirm the conclusions of ref. [1].

5. CONVECTIVE HEAT TRANSFER BETWEEN PARTICLES AND HEAT TRANSFER SURFACE

Convective heat transfer in packed beds

The model for the particle-to-wall heat transfer takes the particles as stationary until displaced by a bubble. Since the particles are near the wall or touch it, their mobility is limited. Thus a packed bed model would apply although detailed analysis requires a close knowledge of the particle packing arrangement and voidage. At high Reynolds numbers in packed beds it has been found that the conduction heat transfer from the wall to the first row of particles is augmented by convection set up by lateral mixing of the gas.

A simple order of magnitude calculation can be used to establish the limit of the influence of gas convection in the region near the point of contact between the particle and the wall. As illustrated in Fig. 3, the gas flow near the contact point is modelled as flow between parallel plates of length l_0 separated by w_0, with l_0 and w_0 dependent upon particle diameter and the angular length in the flow direction of the region considered, ϕ. Spacing w_0 has been chosen as an extreme rather than

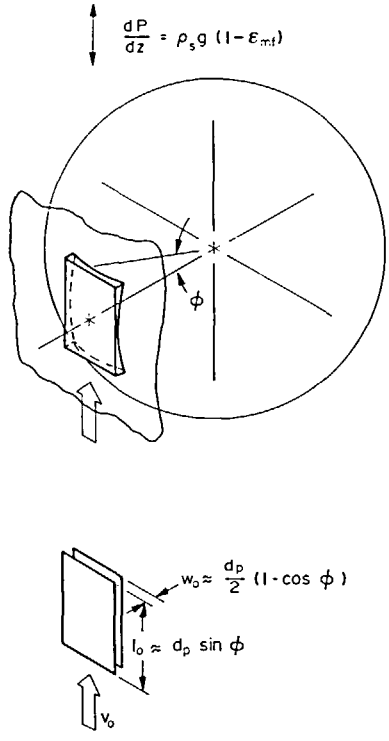

FIG. 3. Geometry of contact point region for estimating local convective effects: (a) pictorial view; (b) parallel plate model.

an average value of the particle–wall separation over the region, thereby ensuring an upper limit for convective effects. The pressure gradient imposed on the model by the surroundings is taken as $\rho_s g\,(1-\varepsilon_{mf})$. Neglecting entrance effects and variations in the lateral direction, the model is equivalent to flow between infinite parallel plates, and gas velocity v_0 can be calculated. With the wall at temperature T_w and the particle at temperature T_p, the gas entering at temperature T_B rapidly reaches a fully developed temperature profile. The rate of energy transport associated with the flux of gas through the channel,

$$\rho v_0 w_0 c\left[T_B - \frac{(T_w+T_p)}{2}\right]$$

can be compared with the conduction across the channel with stagnant gas

$$\frac{k_g l_0}{w_0}(T_p - T_w).$$

Even with this upper bound estimate of the gas convection, it is found that for an included angle, 2ϕ, of 50° the conduction heat transfer through stagnant gas is at least one order of magnitude greater than the gas convection. Using the particle-to-surface conduction model developed earlier [1], it is estimated that 75–85% of the total conduction heat transfer takes place within the included angle, 2ϕ, of 50°. Thus convective effects do not have a first order effect on the conductive heat transfer given by equation (4) and shown in Fig. 2. In addition, in the larger voids between the particles where lateral mixing takes place, direct particle-to-wall conduction is negligible. Thus it follows that the two phenomena, particle-to-surface conduction and lateral mixing are essentially independent of each other and their effect on overall heat transfer is additive since they act independently and in parallel. (It should be noted that this is strictly true only for particles touching, or very nearly touching, the wall: packing irregularities may hold some particles at an intermediate distance from the surface for which the conduction and lateral mixing may be interdependent.)

A number of investigators have measured the overall wall resistance for packed beds. Figure 4 shows the data of three investigators replotted to show only the convective component assuming that the convection and conduction effects act in parallel. The techniques of Yagi and Wakao [11], and Plautz and Johnstone [12] did not allow tests to be run at zero flow, thus the convection component must be found by extrapolation. At progressively higher Reynolds numbers, any error due to this extrapolation will become minimal. For Reynolds numbers less than 2000 the form of the correlation suggested by Yagi and Kunii [13] can be used to represent all of the data,

$$(Nu)_{conv} = 0.05\,RePr, \quad Re \leqslant 2000. \tag{5}$$

From his experimental results, Baskakov [14] correlated the convective augmentation as

$$(Nu)_{conv} = 0.009\,Ar^{1/2}\,Pr^{1/3}. \tag{6}$$

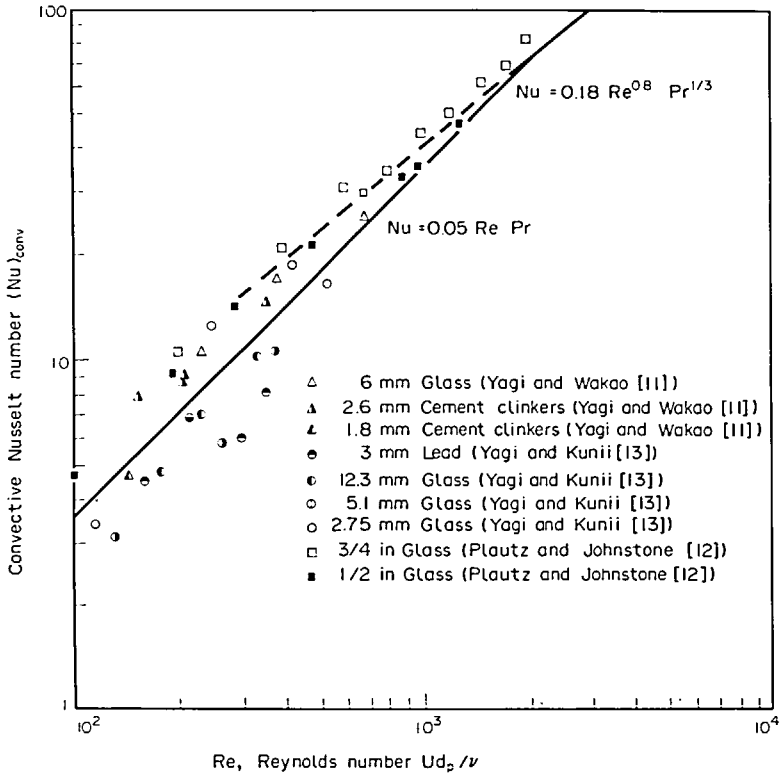

FIG. 4. Convective Nusselt number for heat transfer at walls of packed beds.

The difference between equations (5) and (6) is 16% or less for Re between 200 and 2500. At higher Reynolds numbers, results for turbulent flow through packed beds and channels indicate that the power of the Reynolds number should be reduced. The higher Reynolds number results of Plautz and Johnstone on Fig. 4 suggest the following correlation:

$$(Nu)_{conv} = 0.18\,Re^{0.8}\,Pr^{1/3}, \quad Re > 2000. \qquad (7)$$

Since all of the gases used had values of Pr near unity, the exact influence of the Prandtl number cannot be confidently set.

Adams and Welty [15] have developed a model for the convective augmentation for particles with diameters of 2 mm or greater at gas velocities near the minimum fluidizing velocity. At present the model cannot be generalized since it requires as input the specification of the interstitial turbulence intensity level, the voidage distribution and the particle spacing near the heat transfer surface.

6. RELATIONSHIP BETWEEN PACKED AND FLUIDIZED BEDS

The heat transfer coefficient given by equations (5) and (7) represents the convective heat transfer between packed bed particles adjacent to the wall and the wall itself. It is caused by the motion set up as the fluid flows over and between the particles. If the particle packing next to the wall for a dense phase of a fluidized bed is similar to the packed bed the convective heat transfer coefficient at the wall should be similar. To clarify this point it is important to understand the relationship between heat transfer in a packed bed and heat transfer in a fluidized bed. Consider the case of large particles in a fluidized bed with good particle mixing so that the particle residence time is much less than the particle thermal time constant. The conditions in the fluidized bed are shown on the top of Fig. 5. All of the particles in the bed including those adjacent to the heat transfer surface remain at T_B, the bed temperature. The sole resistance to the heat transfer occurs at the interface between the wall and the first row of particles. The electrical analogy of the heat transfer in the fluidized bed is also shown. The heat transfer is made up of conduction and convection acting in parallel at the interface.

For the packed bed with gas entering the bottom of the bed at T_B and a heat transfer surface at T_w, a diagram of the heat transfer process is shown on the bottom of Fig. 5. As the gas flows over the surface, it is cooled and a region of reduced gas temperature (for $T_B > T_w$) develops analogous to a thermal boundary layer for a single phase heat transfer. As such, the boundary layer represents a resistance to heat transfer between the particles adjacent to the heat transfer surface and the bed at T_B. Due to the boundary layer resistance, the particles adjacent to the surface are at T_l, an

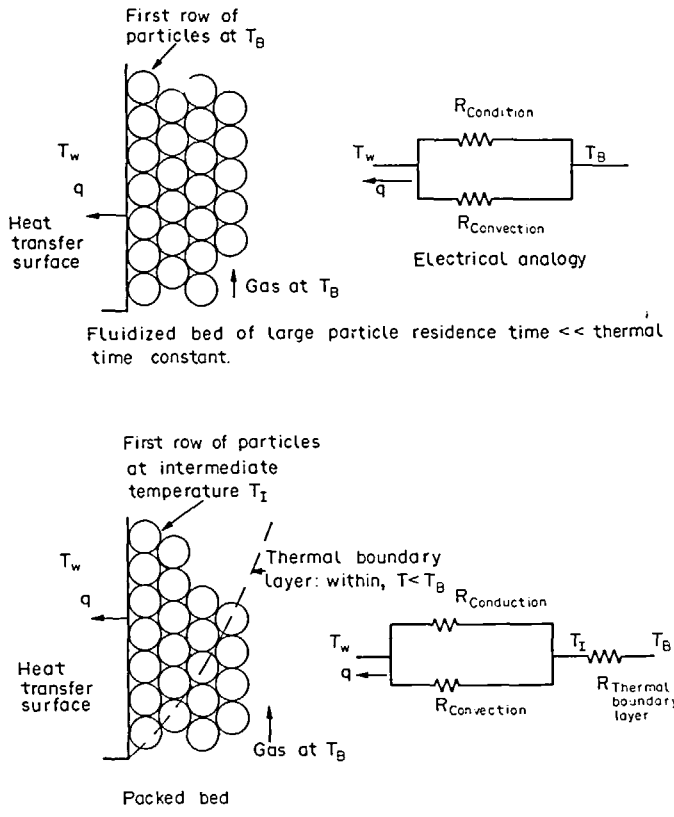

FIG. 5. Comparison of heat transfer mechanisms: fluidized bed of large particles and packed bed.

intermediate temperature between T_w and T_B. There still is a heat transfer resistance at the interface between the particles at T_I and the surface. The electrical analogy to the packed bed case is shown in Fig. 5. There are now two thermal resistances in series, the interface and the boundary layer resistances. If the conditions of the particles at the wall are identical for the fluidized and packed bed (e.g. particle packing geometry, particle shape, superficial gas velocity), the interface resistance will be the same. However, the overall heat transfer will be reduced for the packed bed due to the additional resistance of the thermal boundary layer.

At the minimum fluidization conditions in which bubbles are not present to replace particles at the surface, a packed bed analysis still applies. Thus, the overall heat transfer coefficient for a bed at minimum fluidization cannot be directly related to heat transfer in a vigorously bubbling bed. The heat transfer coefficient at minimum fluidization is decreased due to the added resistance of the thermal boundary layer which is not present in a bubbling bed. The thermal boundary layer resistance will vary with the geometry of the heat transfer surface, especially the vertical length as well as other factors which may be unimportant for heat transfer in a vigorously fluidized bed.

It can be seen in Fig. 4 that the convective heat transfer coefficient at the wall is approximately the same for several experiments with different packed bed geometries. In addition, fluidized beds with large particles, where the interface resistance is dominated by convection, show no sudden change in the overall heat transfer coefficient between packed and minimally fluidized states. It follows that convection heat transfer at the wall is not significantly influenced by changes in particle geometry and changes from the packed to fluidized state. Thus, for the emulsion phase of a fluidized bed the convective heat transfer at the wall should be the same as that for a packed bed and equations (5) and (7) apply for fluidized beds.

On the other hand, in packed bed experiments the conductive heat transfer coefficient between the wall and first row of particles tended to vary widely with particle size and bed geometry [11–13]. The conductive component is sensitive to local packing and one cannot confidently extend the similarity between packed and fluidized beds to the conductive component at the wall.

In the packed bed experiments the Reynolds number for convection is based on the superficial velocity through the bed. For a fluidized bed at minimum fluidization, the minimum fluidization velocity, U_{mf}, should be used in the Reynolds number given in equations (5) and (7). Contact between emulsion phase particles and the heat transfer surface should constrain particles adjacent to the surface until they are displaced by the action of a bubble. As the superficial velocity is increased above the U_{mf}, and the bubble voidage

increases, the gas flow associated with the emulsion can increase, e.g. in the emulsion phase near a void. The average superficial velocity in the emulsion phase of a 3-dim. bed with stationary bubbles becomes [16]

$$U = (1+2\delta)U_{mf}. \quad (8)$$

The velocity given by equation (8) will be used in the Reynolds number in equations (5) and (7). We will also assume that the local bubble voidage near the heat transfer surface is the same magnitude as the average bubble voidage in the bed. The present model should apply to the turbulent flow regime since there still are numerous particle contacts with the wall. In this case, where the gas phase is more likely to be the continuous phase, the superficial velocity should be used in the expression for the Reynolds number. In other words, while the particle is at the wall the slip velocity is assumed to be the superficial velocity.

The overall heat transfer rate between the emulsion and the wall for large particles is the sum of the conductive and convective components. Thus, the emulsion phase heat transfer becomes, for Reynolds number less than 2000,

$$\left(\frac{hd_p}{k_g}\right)_{\text{Emulsion}} = 12+0.05(1+2\delta)\frac{U_{mf}}{\nu}d_p Pr. \quad (9)$$

This holds for fluidized beds of 'large' particles in which the particle residence time at a heat transfer surface is less than the particle thermal time constant. For irregular shaped particles with sphericity much less than unity, it is estimated that the conduction constant, the first term on the RHS of equation (9) should be halved from 12 to approximately 6.

7. HEAT TRANSFER FROM BUBBLES TO WALL

When the surface is covered by a bubble or void, gas flows through the bubble and single phase convective heat transfer occurs. In bubbly flow the gas velocity through a bubble in the middle of the bed is $3U_{mf}$.

The bubble rise velocity can be found from the two-phase hypothesis

$$U = \delta U_b+(1+2\delta)U_{mf}. \quad (10)$$

The gas phase convection associated with the bubble may be estimated using the Pohlhausen solution for heat transfer in a laminar boundary layer on a flat plate [17],

$$\left(\frac{hd_p}{k_g}\right)_{\text{void}} = 0.664\left[\frac{(U_b+3U_{mf})d_p}{\nu}\right]^{0.5} Pr^{0.33}\left(\frac{d_p}{L}\right)^{0.5}. \quad (11)$$

To be conservative, for horizontal tubes L, the average bubble length, will be taken as one-quarter of the tube circumference.

For horizontal tubes, there is a defluidized region at the bottom; the heat transfer should be similar to single phase flow near the stagnation point of a cylinder. The solution for this case differs from equation (11) by 10% at most. Thus equation (11) can be used for both regions. At the top of a horizontal tube a partially stagnant layer of particles often forms. If the residence time of this layer is larger than the thermal time constant of the particles, the present results will overestimate the heat transfer.

8. OVERALL HEAT TRANSFER

To obtain an overall heat transfer coefficient for large particle fluidized beds, the expressions for each region must be combined. The overall heat transfer can be expressed as,

$$\left[\frac{hd_p}{k_g}\right]_{\text{overall}} = (\delta)\left[\frac{hd_p}{k_g}\right]_{\text{void}}+(1-\delta)\left[\frac{hd_p}{k_g}\right]_{\text{emulsion}}. \quad (12)$$

For Reynolds numbers less than 2000 with spherical particles this can be replaced by

$$\left[\frac{hd_p}{k_g}\right]_{\text{overall}} = \delta\left[\frac{hd_p}{k_g}\right]_{\text{void}} +(1-\delta)\left[12+0.05(1+2\delta)\frac{U_{mf}d_p}{\nu}Pr\right]. \quad (13)$$

For a horizontal tube with a bubble fraction, or δ, of 0.3 or less over the tube circumference, the contribution of the bubble phase heat transfer for particles smaller than 4 mm is less than 15% of the total heat transfer at atmospheric pressure. Note that the present expressions hold for heat transfer surfaces of various shapes as long as the particles can be considered 'large' as defined here.

9. RADIATION HEAT TRANSFER

For a large particle fluidized bed, radiation can be handled in a very straightforward fashion. Since the particles adjacent to the tube surface are at approximately T_B, radiation acts independently of conduction and convection. The radiative heat transfer is simply that between two isothermal parallel planes at T_w and T_B and the radiative flux can be added to that calculated for conduction and convection. However, the effective emissivity of the particles is larger than their surface emissivity due to the re-entrant geometry between particles.

This simplification does not apply to smaller particle fluidized bed heat transfer since the particles in radiant communication with the surface are those near the surface and their temperature is significantly reduced during their residence period. The radiant cooling of the particles reduces the conductive and convective flux and vice versa. Radiation is not simply additive to the other modes of heat exchange for small particles. Again, the large particle criterion can be used to determine when the simplified form of the radiative flux is appropriate.

10. PREDICTED TRENDS

The model of the heat transfer developed in previous sections of the paper can be used to predict the influence of each of the important variables. This is shown in Fig. 6 using the heat transfer coefficient divided by the fraction of surface covered by emulsion. For relatively small particles h is inversely proportional to d_p. For larger particles, convective mixing becomes important to the point where h increases with d_p. The convective effect is also responsible for the increase in h at elevated pressure with large particles. As the bed temperature is raised, radiation becomes important and the thermal conductivity of the air increases. The results shown in Fig. 6 should be used with care for particle diameters less than 1 mm since the particles are assumed to remain at the bed temperature during their residence at the heat transfer surface. This will require residence times less than 1 s and very vigorously fluidized beds. Thus the results represent an upper limit for the particle-to-surface heat transfer. Effects of particle shape are also included in the figure. This should primarily affect the conduction contribution of the interface heat transfer. At this time quantitative information covering this effect is only approximate.

11. EXPERIMENTAL RESULTS

Instantaneous heat transfer coefficient

Instantaneous heat transfer data will provide a good means to evaluate the accuracy of the proposed large particle model. The maximum and minimum values of the instantaneous heat transfer coefficient at one location of the surface will correspond to conditions in which the surface is covered by a group of particles and a bubble, respectively.

Catipovic [3] recently completed measurements of instantaneous and time averaged heat transfer around the circumference of horizontal tubes 5 cm in diameter. Very fast response heat transfer probes were used; even for small particles the maximum measured heat transfer coefficient should respond to the interfacial resistance alone. Figure 7 shows a comparison of Catipovic's maximum and minimum values with those values predicted in the present work. Particles with a diameter of 2 mm and less had a sphericity of 0.85 and below and will be considered irregular. Particles 2.85 mm and larger in diameter had sphericity of 0.95 and above and will be considered spherical.

The minimum instantaneous heat transfer coefficients at the sides of the tubes, under bubbles, should be very close to the value at the stagnation point. In the experiments, minimum values remained approximately the same around the entire tube circumference and agreed closely with the predicted values.

The maximum instantaneous values were found to vary considerably around the circumference although differences between single tubes and tube banks were slight. Figure 7 shows both the maximum instantaneous values found on the tube and the circumferential average of the maximum values. Theoretical values of the emulsion heat transfer coefficient are shown for a bubble voidage of 0 and 0.25. The latter represents an average of the maximum bubble voidage found in the bed. The maximum values of heat transfer coefficient data tend to follow a transition from the smooth to the

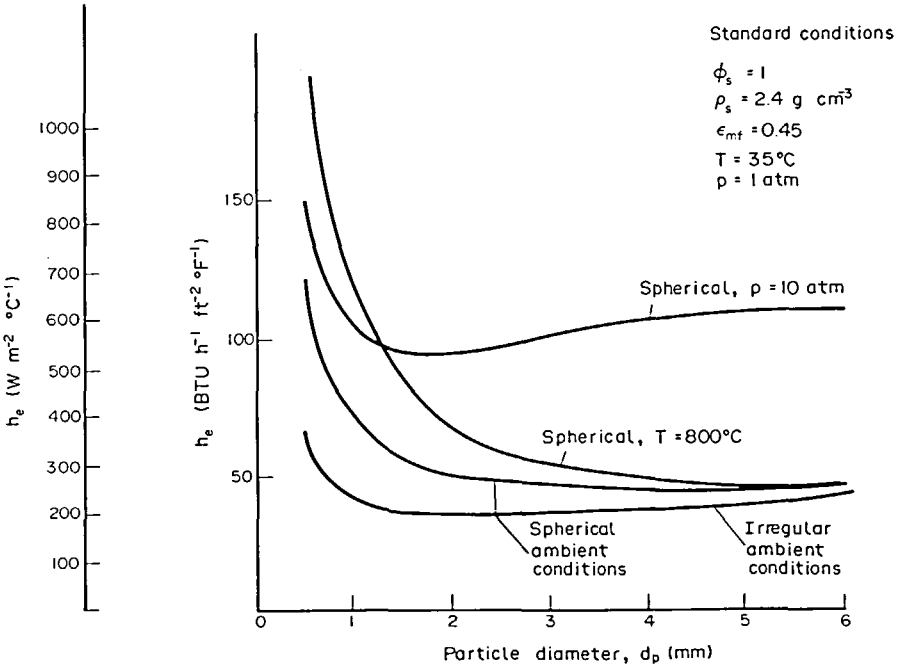

FIG. 6. Heat transfer coefficient vs particle diameter, influence of temperature level, pressure level, and particle sphericity.

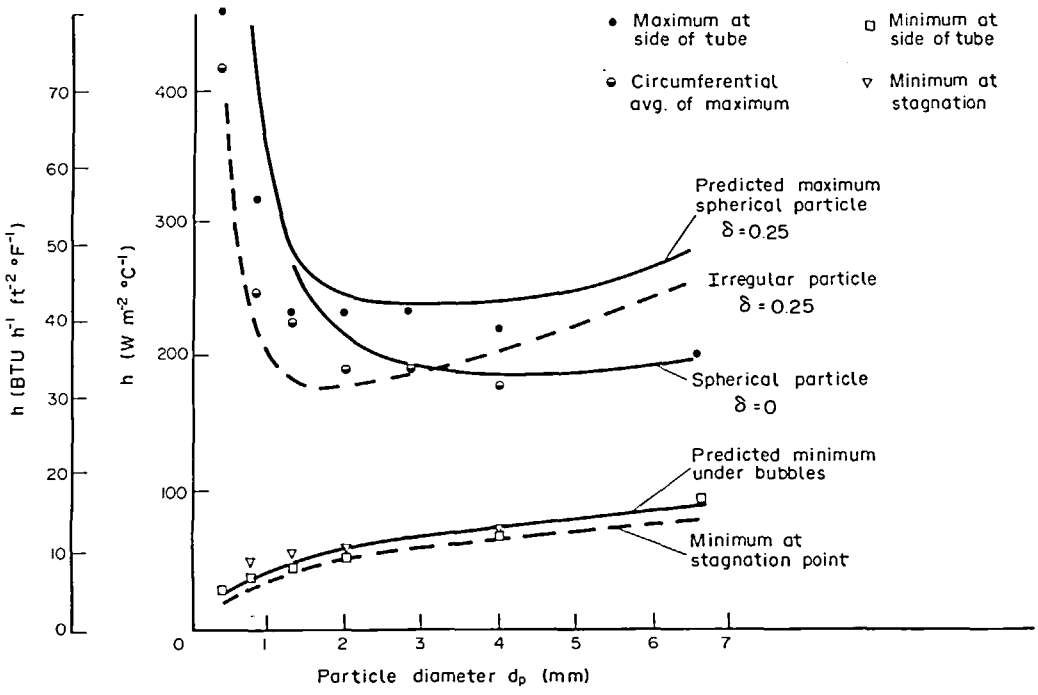

FIG. 7. Maximum and minimum heat transfer coefficients, experimental data from Catipovic [3].

irregular model as particle size is reduced and the particle sphericity also is reduced. The result of 6.6 mm is an anomaly, probably due to the large ratio of the particle to tube diameter, approximately one-eighth.

12. AVERAGE HEAT TRANSFER COEFFICIENTS

Results for time averaged and surface averaged heat transfer coefficients for large particles have been measured by several investigators for horizontal tubes. To compare the proposed model to the measurements, the voidage, δ, must be known. It will be assumed that the voidage near the tubes is equal to the average bed voidage.

Figures 8 and 9 illustrate the comparison of the predicted overall heat transfer coefficients and the overall values measured by Catipovic. These comparisons are made only for that heat transfer data which was accompanied by data of bubble fraction δ. Catipovic also measured the emulsion contact time fraction at his heated tube surface, which may be regarded as more representative of local voidage conditions at the surface. This quantity, unfortunately, is difficult to measure and few other researchers have pursued it.

For a given particle size, the average heat transfer coefficient does not change appreciably over a wide range of superficial velocities. The convective

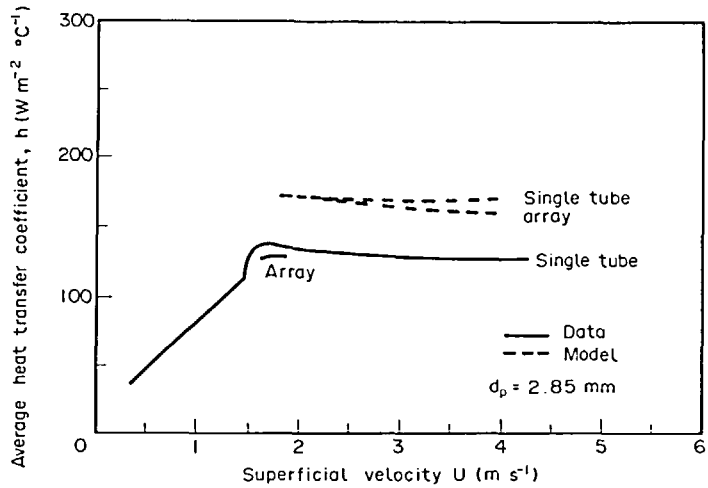

FIG. 8. Average heat transfer coefficients; experimental data of Catipovic [3] compared with the model.

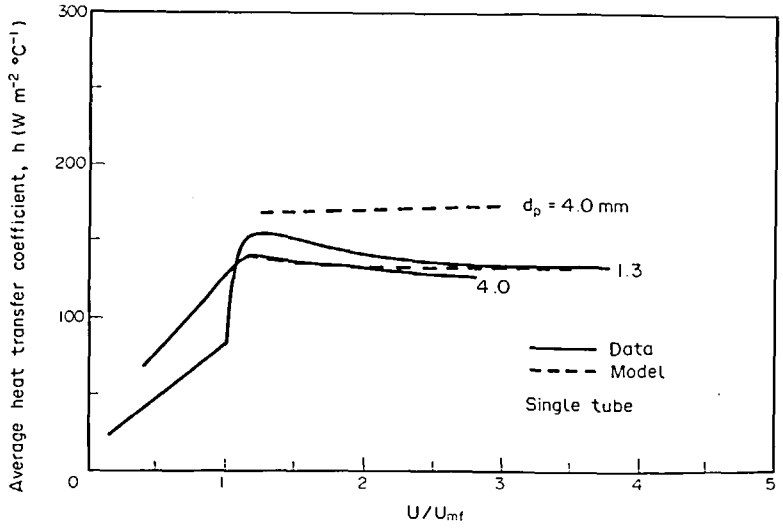

FIG. 9. Average heat transfer coefficients; experimental data of Catipovic [3] compared with the model.

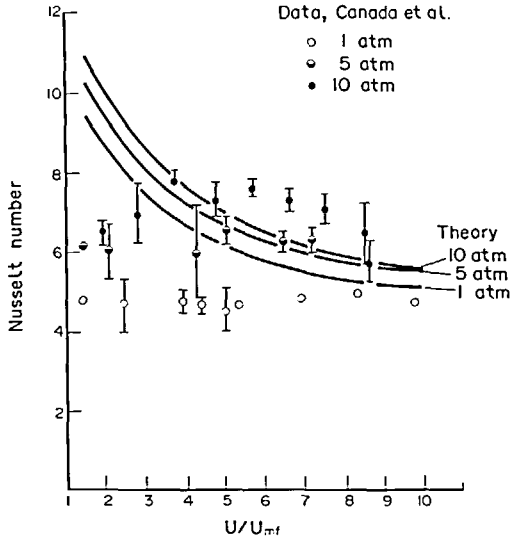

FIG. 10. Effect of pressure on heat transfer coefficients of 650 μm particles; data of Staub *et al.* [18].

component of the emulsion heat transfer increases with δ, while the fraction of the surface covered by emulsion decreases with δ. These two trends tend to balance each other. Figure 8 shows that the model overpredicts the heat transfer coefficient of the 2.85 mm material by about 30%. Figure 9 shows an overprediction for the 4.0 mm material but a fairly close fit for the data of the 1.3 mm particles. Some of the disagreement may be due to stagnant particles on top of the tubes which are not explicitly accounted for in the model. The 2.85 and 4.0 mm dolomite particles had sphericities of 0.95 and 0.97, respectively, and were considered smooth. The 1.3 mm quartz sand particles, however, had a sphericity of 0.82 and were here assumed to be irregular. The conduction Nusselt number for these rough particles was taken to be 6.0 instead of 12. Despite the apparent error in magnitude, the variation of the heat transfer coefficient with superficial velocity is closely followed by the model. Figure 10 shows data taken by Staub *et al.* [18] for 650 μm spherical particles at pressures between 1

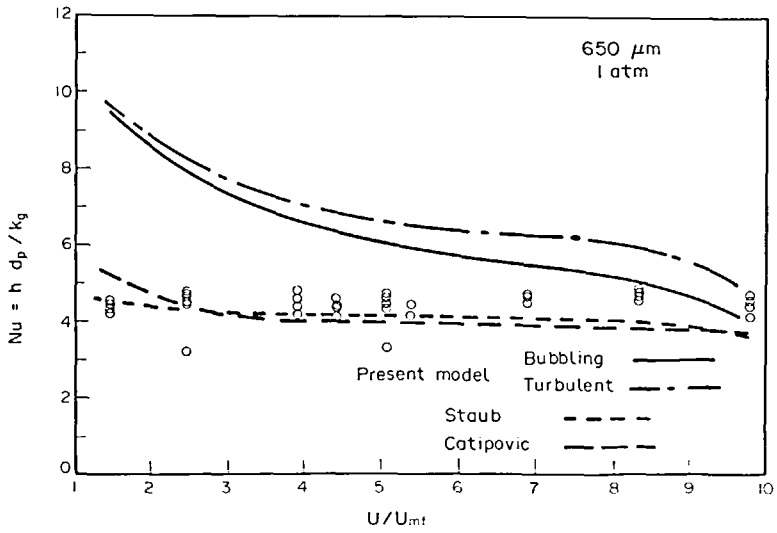

FIG. 11. Average Nusselt number variation with superficial velocity; data of Staub *et al.* [18] compared with four models: 650 μm particles at 1 atm.

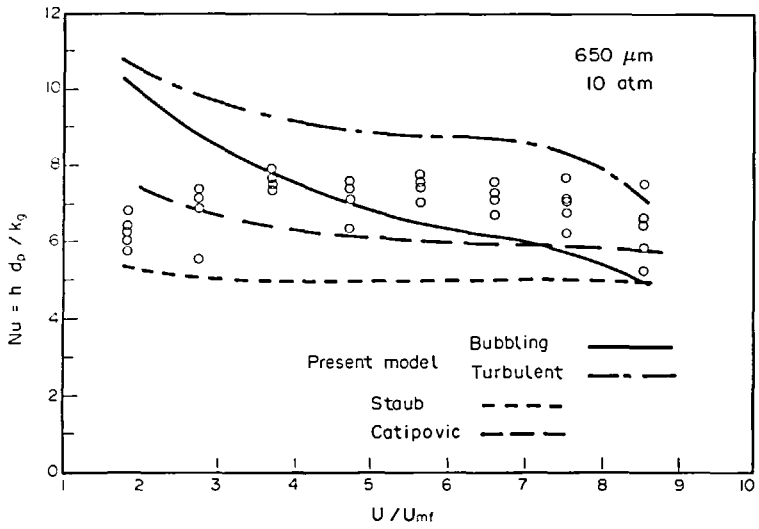

FIG. 12. Average Nusselt number variation with superficial velocity; data of Staub *et al.* [18] compared with four models: 650 μm particles at 10 atm.

and 10 atm. The predicted values use the measured bed expansion for the bubble fraction. The present model represents an upper bound upon the heat transfer coefficient. At low values of U/U_{mf} the frequency of particle replacement is not adequate for the particles at the wall to remain isothermal. At higher values of U/U_{mf}, such a condition is met and agreement is very good. Note the modest influence of pressure level on the small particles.

Figures 11 and 12 compare the model predictions with data of Staub *et al.* for the 650 μm glass at 1 and 10 atm., respectively. The present model is compared to the correlation of Catipovic and the mixing length model of Staub on Figs. 11 and 12. Since many of the experimental results presented by Staub *et al.* were reported to be in the turbulent flow regime, these figures display the predictions of the model for both bubbling and turbulent fluidization. The distinction made here is that for turbulent fluidization, the superficial velocity is used in estimating the gas convective component of the emulsion phase heat transfer.

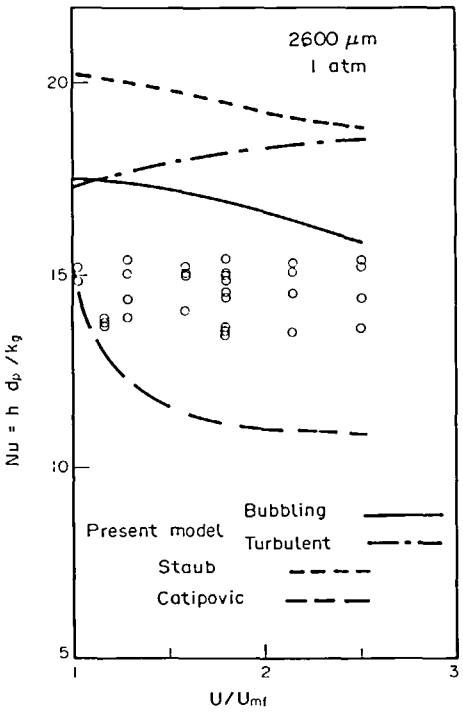

FIG. 13. Average Nusselt number variation with superficial velocity; data of Staub *et al.* [18] compared with four models: 2600 μm particles at 1 atm.

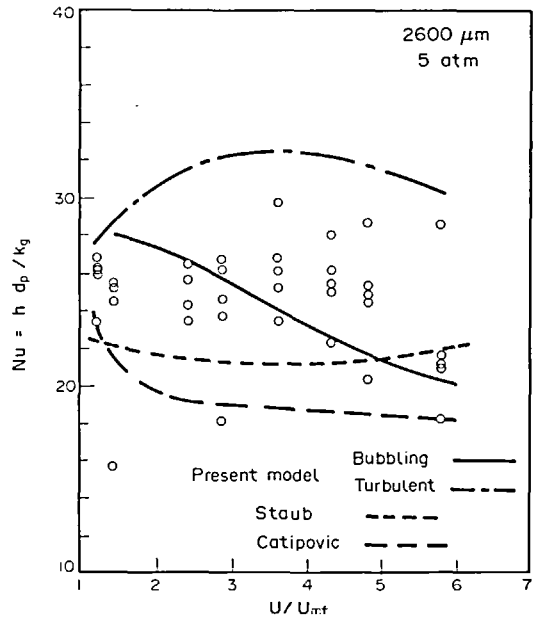

FIG. 14. Average Nusselt number variation with superficial velocity; data of Staub *et al.* [18] compared with four models: 2600 μm particles at 5 atm.

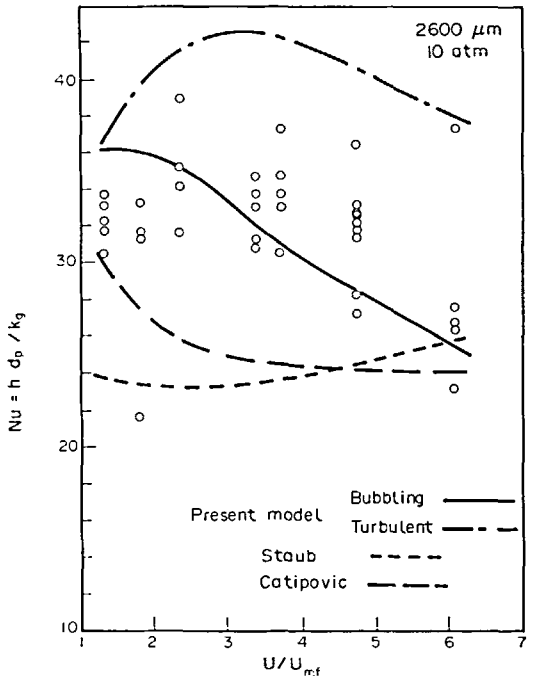

FIG. 15. Average Nusselt number variation with superficial velocity; data of Staub *et al.* [18] compared with four models: 2600 μm particles at 10 atm.

Figures 13–15 show the comparison between the model and the large particle (2600 μm) data of Staub *et al.* for 1, 5 and 10 atm., respectively. Again the Catipovic and Staub models are included; at increasing pressures the latter models give progressively worse agreement with the data. Reasonable agreement between the model and data of Chandran *et al.* [19] is shown in Fig. 16. The greater disparity at low superficial velocities is due to lower bubbling rates and longer residence times which allow the particle temperature to change appreciably while contacting the surface.

Data of Botterill and Denloye [20] for maximum heat transfer coefficients (measured for two size ranges of sand at several bed pressures) are compared with the model in Fig. 17. If the particles are taken to be rough, the model fits the data well.

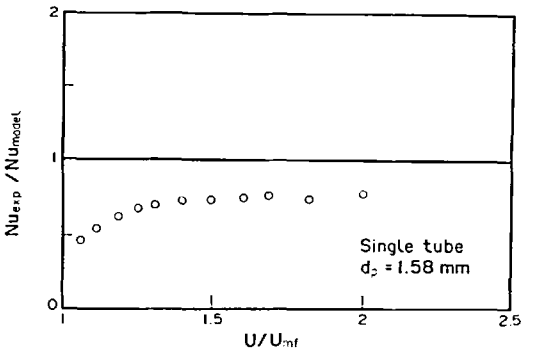

FIG. 16. Ratio of Chandran's experimental data [19] to model prediction of average Nusselt number; 1580 μm particles.

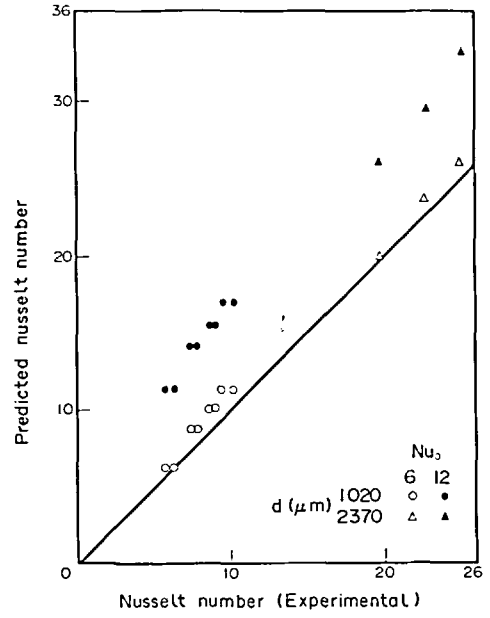

FIG. 17. Comparison of predicted Nusselt number with experimental results of Denloye and Botterill [20].

13. CONCLUSIONS

A new physical model for large particle fluidized bed heat transfer has been developed which gives good agreement with local and average heat transfer results of a number of investigators.

For large particles in a bubbling bed, the particles adjacent to the heat transfer surface remain at the bulk bed temperature and the frequency of particle replacement does not influence the results.

For large particles, the heat transfer resistance is concentrated in the interface between the surface and the first row of particles. In the interface, heat transfer by conduction, convection and radiation all act in parallel. Conduction takes place through the gas film near the contact point of the particle on the surface. The convective heat transfer coefficient can be found from the interfacial convective coefficient measured for packed beds. At minimum fluidization of large particles, the overall heat transfer coefficient is less than the value for a bed at higher superficial velocities. The decrease is due to the presence of an additional heat transfer resistance of a thermal boundary layer which extends into the bed beyond the particles adjacent to the surface. When the bed is bubbling or well stirred, the thermal boundary layer is not present. Thus, heat transfer coefficients at minimally fluidized conditions cannot be directly related to coefficients at higher superficial velocities; the overall results at minimum fluidization can be directly related to results at lower velocities, in packed beds, where the thermal boundary layer does exist.

Acknowledgements—The work reported by the authors was done under sponsorship by the United States Department of Energy and the National Science Foundation.

REFERENCES

1. N. A. Decker and L. R. Glicksman, Conduction heat transfer at the surface of bodies immersed in gas fluidized beds of spherical particles, *A.I.Ch.E. Symp. Ser.* 77 (208), 341–349 (1981).
2. R. R. Cranfield and D. Geldart, Large particle fluidisation, *Chem. Engng Sci.* **29**, 935 (1974).
3. N. M. Catipovic, Heat transfer to horizontal tubes in fluidized beds: experiment and theory, PhD Thesis, Department of Chemical Engineering, Oregon State University (1979).
4. J. C. Chen, Heat transfer to tubes in fluidized beds, ASME paper No. 76-HT-75 (1975).
5. R. Chandran, Local heat transfer and fluidization dynamics around horizontal tubes in fluidized beds, PhD Dissertation, Lehigh University, Bethlehem, PA (1980).
6. N. I. Gelperin and V. G. Einstein, Heat transfer in fluidized beds, in *Fluidization* (edited by J. F. Davidson and D. Harrison). Academic Pfess, London (1971).
7. E. U. Schlünder, Warmeubergang an bewegte Kugelschuttungen bei kurzfristigem Kontakt, *Chemie–Ingr–Tech.* **43**, 651 (1971).
8. J. S. M. Botterill and J. R. Williams, The mechanism of heat transfer to gas-fluidized beds, *Trans. Inst. Chem. Engrs* **41**, 217 (1963).
9. J. D. Gabor, Wall-to-bed heat transfer in fluidized and packed beds, *Chem. Engng Progr. Symp. Ser.* **66** (105), 76 (1970).
10. D. Gloski, An experimental study of the transient particle–wall thermal contact resistance in fluidized and packed beds, M.S. Thesis, Department of Mechanical Engineering, MIT (1981).
11. S. Yagi and N. Wakao, Heat and mass transfer from wall to fluid in packed beds, *A.I.Ch.E. Jl* **5**, 79–85 (1959).
12. D. A. Plautz and H. F. Johnstone, Heat and mass transfer in packed beds, *A.I.Ch.E. Jl* **1**, 193–99 (1955).
13. S. Yagi and D. Kunii, Studies on heat transfer near wall surface in packed beds, *A.I.Ch.E. Jl* **6**, 97–104 (1960).
14. A. P. Baskakov, O. K. Vitt, V. A. Kirakosyan, V. K. Maskaev and N. F. Filippovsky, Investigation of heat transfer coefficient pulsations and of the mechanism of heat transfer from a surface immersed in a fluidized bed, in *La Fluidisation et ses Applications*, pp. 293–302. Soc. Chim. Ind. (1974).
15. R. L. Adams and J. R. Welty, A gas convection model of heat transfer in large particle fluidized beds, *A.I.Ch.E. Jl* **25**, 395 (1979).
16. J. A. Valenzuela and L. R. Glicksman, Gas flow distribution in a bubbling fluidized bed, presented at A.I.Ch.E. 74th Annual Meeting, Fundamentals of Fluidization and Fluid Particle Systems, New Orleans (1981).
17. W. M. Kays, *Convective Heat and Mass Transfer.* McGraw-Hill, New York (1966).
18. F. W. Staub, R. T. Wood, G. S. Canada and M. N. McLaughlin, Two phase flow and heat transfer in fluidized beds, Final Technical Report to E.P.R.I., Report SRD-78-103, General Electric, Schenectady, New York (1978).
19. R. Chandran, J. C. Chen and F. W. Staub, Local heat transfer coefficients around horizontal tubes in fluidized beds, *J. Heat Transfer* **102**, 152 (1980).
20. A. E. Denloye and J. S. M. Botterill, Bed to surface heat transfer in a fluidized bed of large particles, *Powder Tech.* **19**, 197 (1978).

TRANSFERT THERMIQUE DANS LES LITS FLUIDISES A GROSSES PARTICULES

Résumé—Un modèle basé sur la physique est proposé pour le transfert thermique à des surfaces immergées dans des lits fluidisés à grosses particules. Celles-ci se distinguent par des constantes de temps sensiblement plus grandes que leur temps de séjour à la surface d'échange thermique. Dans les conditions opératoires d'un foyer à lit fluidisé, sont "larges" les particules d'un millimètre ou plus. La conduction avec le gaz près des points de contact solide et la convection par l'écoulement intersticiel contribuent au transfert thermique pendant le contact de l'émulsion (ou phase dense). Quand la taille de la particule augmente le transfert thermique par la convection crée un plus grand transfert global. On montre que la composante de convection du gaz n'est pas simplement reliée à la convection globale dans un lite fixe ou légèrement fluidisé. Le modèle montre un bon accord avec les données en provenance de plusieurs sources.

WÄRMETRANSPORT IN FLIESSBETTEN MIT GROSSEN PARTIKELN

Zusammenfassung—Es wird ein physikalisch begründetes Modell für den Wärmetransport an den eingetauchten Oberflächen in Fließbetten mit großen Partikeln vorgeschlagen. Als große Partikel werden solche bezeichnet, deren thermische Zeitkonstante wesentlich größer als ihre Verweilzeit an einer Wärmeaustauschfläche ist. Unter den typischen Betriebsbedingungen einer Feuerung nach dem Fließbettverfahren sind demnach Partikel von 1 mm Größe und mehr als groß zu bezeichnen. Sowohl die Wärmeleitung des Gases an Berührungspunkten der Partikel als auch die Konvektion des strömenden Gases in den Zwischenräumen tragen zum Wärmetransport während des Schichtkontaktes (oder in der dichten Phase) bei. Mit zunehmender Partikelgröße wächst der Anteil der Gaskonvektion am Wärmeübertragungsvorgang. Es wird gezeigt, daß der Anteil der Gaskonvektion im Fließbett nicht in einfacher Weise mit der gesamten Gaskonvektion in einem Festbett oder einem ruhenden Fließbett zusammenhängt. Das Modell liefert gute Übereinstimmung mit Daten verschiedener Quellen.

ТЕПЛОПЕРЕНОС В ПСЕВДООЖИЖЕННЫХ СЛОЯХ КРУПНЫХ ЧАСТИЦ

Аннотация—Предложена физически обоснованная модель для расчета теплопереноса к поверхностям, погруженным в псевдоожиженные слои крупных частиц. «Крупными» считаются такие частицы, значения тепловых временных констант для которых значительно превышают время их пребывания на поверхности теплообмена. При обычных рабочих режимах в камере сгорания с псевдоожиженным слоем частицы размером 1 мм и выше считаются «крупными». Передача тепла теплопроводностью через газ у точек контакта частиц и конвекцией за счет течения газа в зазорах между ними усиливают теплоперенос. При увеличении размера частиц доля переноса тепла за счет конвекции возрастает. Отмечен сложный характер зависимости доли конвективного переноса тепла от конвекции газа в плотном или устойчиво псевдоожиженном слое. Показано, что модель хорошо согласуется с данными других авторов.